

Communication

# Intermolecular Interactions Drive the Unusual Co-Crystallization of Different Calix[4]arene Conformations

Dominic Taylor<sup>1</sup>, Irene Ling<sup>2</sup>, Filipe Vilela<sup>1,\*</sup> and Scott J. Dalgarno<sup>1,\*</sup> 

<sup>1</sup> School of Engineering and Physical Sciences, Heriot-Watt University, Riccarton, Edinburgh EH14 4AS, UK; dt121@hw.ac.uk

<sup>2</sup> School of Science, Monash University Malaysia, Jalan Lagoon Selatan, 47500 Bandar Sunway, Malaysia; ireneling@monash.edu

\* Correspondence: f.vilela@hw.ac.uk (F.V.); s.j.dalgarno@hw.ac.uk (S.J.D.)

**Abstract:** Crystallization of 5,17-dibromo-11,27,23,25-tetraone-26,28-dipropoxycalix[4]arene results in the rare observation of two different calix[4]arene conformations (partial cone and 1,3-alternate) co-crystallized within the same single crystal X-ray structure. Analysis using <sup>1</sup>H and <sup>13</sup>C NMR spectroscopy revealed that only a single conformation (the cone) was present in solution, and in contrast to the structures of other reported calix[4]arenes and calix[4]quinones, both conformations of the compound present in this crystal structure have a “pinched” shape, drastically reducing Br-Br separation and associated cavity sizes.

**Keywords:** crystal structure; calix[4]quinone; conformation



**Citation:** Taylor, D.; Ling, I.; Vilela, F.; Dalgarno, S.J. Intermolecular Interactions Drive the Unusual Co-Crystallization of Different Calix[4]arene Conformations. *Crystals* **2022**, *12*, 250. <https://doi.org/10.3390/cryst12020250>

Academic Editors: Venu Vangala, Srinivasulu Aitipamula and Olga Kataeva

Received: 11 January 2022

Accepted: 10 February 2022

Published: 12 February 2022

**Publisher's Note:** MDPI stays neutral with regard to jurisdictional claims in published maps and institutional affiliations.



**Copyright:** © 2022 by the authors. Licensee MDPI, Basel, Switzerland. This article is an open access article distributed under the terms and conditions of the Creative Commons Attribution (CC BY) license (<https://creativecommons.org/licenses/by/4.0/>).

## 1. Introduction

Calix[*n*]quinones are a class of macrocyclic molecules that are structurally related to the more widely recognised calix[*n*]arenes, the latter of which have been extensively studied as supramolecular hosts. While they have not been the recipient of the same level of attention as calix[*n*]arenes, calix[*n*]quinones have been investigated for their electrochemical properties [1–3], and potential applications such as cathodic materials in lithium-ion batteries [4]. In addition, calix[*n*]quinones are capable of forming complexes with alkali and alkaline-earth metal ions [5,6], and can be further modified to access a wide range of functionalised calix[*n*]arenes [7].

One property of calix[*n*]arenes that have long been the subject of study is their conformational flexibility, which arises due to the ease of rotation around the methylene bridges. For calix[4]arenes, four well-defined conformations can be described: these are the cone, partial cone, 1,2-alternate, and 1,3-alternate conformations (Figure 1) [8]. These can be described by assigning each of the aromatic groups as projecting up (u) or down (d) relative to an average plane defined by the bridging methylene groups. For example, the cone conformation can be described as having all aromatic rings orientated upwards (uuuu) while the 1,3-alternate conformation is characterised as having an alternating sequence of upwards and downwards groups (udud). For simple calix[4]arenes featuring low degrees of substitution on the lower-rim, interchange between the four conformations occurs readily in solution [9]. However, it is possible to either slow this interchange by partial substitution, mainly by forming alkyl ethers on the lower-rim oxygen atoms, or completely suppress it through exhaustive substitution [10]. Depending upon the reaction conditions selected for lower rim modification, it is possible to lock the calix[4]arene into one of these non-interconverting conformations, or atropisomers. In comparison to calix[4]arenes, the conformational flexibility of calix[4]quinones has not been as thoroughly investigated, although some studies have been performed. For example, calix[4]diquinones, which possess two quinone moieties on opposing sides of the molecule, are more flexible than structurally related 25,27-dialkoxycalix[4]arenes [11].

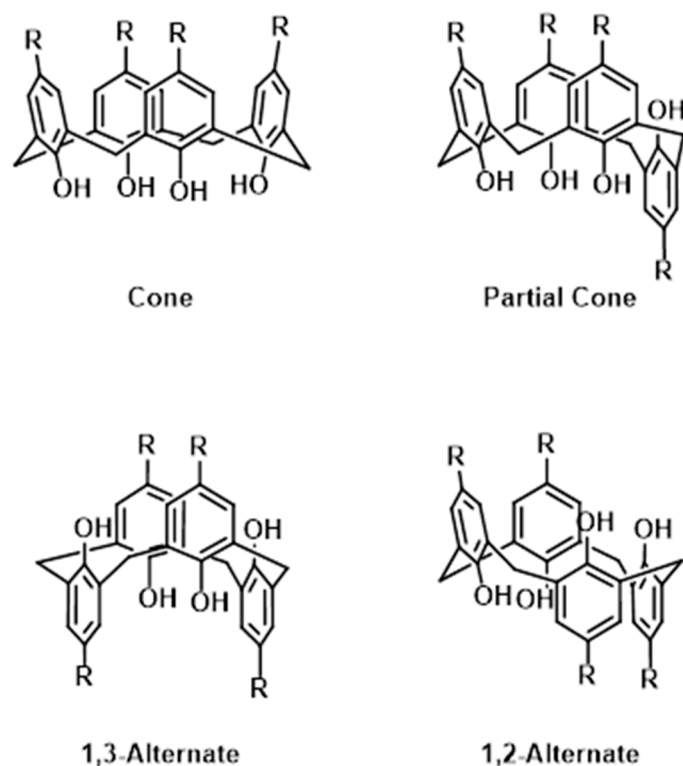
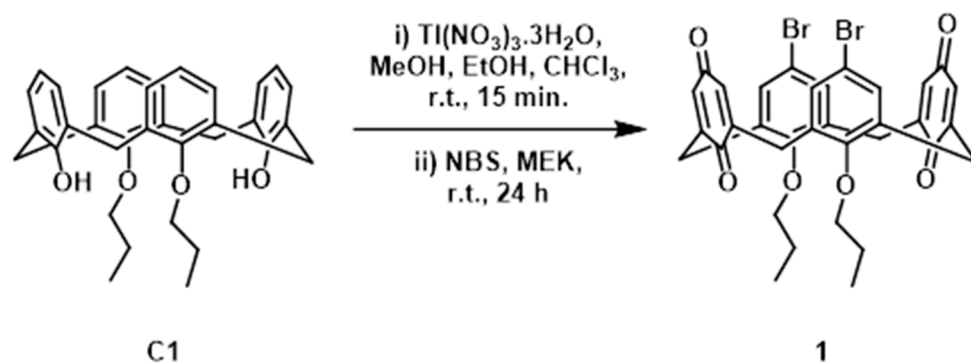


**Figure 1.** Chemical structures of the four conformations of calix[4]arene.

The synthesis of 5,17-dibromo-11,27,23,25-tetraone-26,28-dipropoxycalix[4]arene (**1**) has been previously achieved as shown in Scheme 1 [2], by oxidation of calix[4]arene **C1** to the corresponding *p*-quinone using thallic nitrate [12,13], followed by bromination using *N*-bromosuccinimide (NBS) in butanone (MEK) [14]. However, its crystal structure and conformational behaviour in solution has not yet been reported. Herein we describe the crystal structure of **1**, the asymmetric unit of which contains two distinct conformations of calix[4]diquinone, the partial cone (**1a**) and the 1,3-alternate (**1b**) conformations (Figure 2). This can be contrasted with the solution state where NMR spectroscopic evidence suggests that only a single conformation, the cone conformation (**1c**), is present.



**Scheme 1.** Synthesis of **1** using a method developed by Genorio [2].

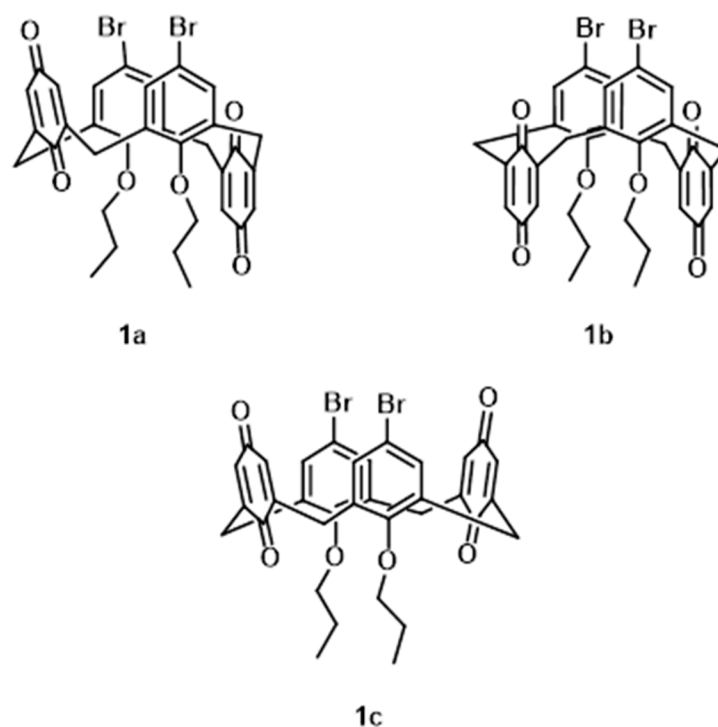


**Figure 2.** Chemical structure of the different relevant conformations of calix[4]quinone **1**.

## 2. Materials and Methods

### 2.1. Synthesis and Characterisation of **1**

The synthesis of compound **1** has previously been reported by Genorio [2].  $^1\text{H}$  NMR (300 MHz, 25 °C,  $\text{CDCl}_3$ )  $\delta_{\text{H}}$  7.01 (s, 2 H), 6.63 (s, 2 H), 3.79 (d, 4 H,  $^2J_{\text{HH}} = 13.1$  Hz), 3.63 (t, 4 H,  $^3J_{\text{HH}} = 7.1$  Hz), 3.27 (d, 4 H,  $^2J_{\text{HH}} = 13.2$  Hz), 1.79 (m, 4 H,  $^3J_{\text{HH}} = 7.3$  Hz), 0.99 (t, 6 H,  $^3J_{\text{HH}} = 7.4$  Hz).  $^{13}\text{C}$  NMR (75.5 MHz, 25 °C,  $\text{CDCl}_3$ ) 188.0 (C), 185.4 (C), 155.8 (CH), 147.0 (CH), 132.8 (C), 132.1 (C), 116.1 (CH), 76.7 ( $\text{CH}_2$ ), 31.7 ( $\text{CH}_2$ ), 23.6 ( $\text{CH}_2$ ), 10.6 ( $\text{CH}_3$ ). IR  $\nu$  ( $\text{cm}^{-1}$ ) 1652 (s, C=O). Yellow crystals suitable for single crystal x-ray diffraction were obtained by slow evaporation of a DCM solution of **1**.

### 2.2. Crystallography

A crystal was coated in paratone-N oil and mounted on a Mitigen cryoloop and mounted on a Bruker D8 Venture diffractometer. Data were collected using the Apex2 suite of programs. The crystal was kept at 100.0 K during data collection. Using Olex2 [15], the structure was solved with the SHELXT structure solution program using Intrinsic Phasing and refined with the SHELXL refinement package using Least Squares minimization [16,17]. Crystallographic data for **1** have been deposited in the Cambridge Crystallographic Data Centre. Crystal Data for **1** (CCDC 2132914):  $\text{C}_{68}\text{H}_{60}\text{Br}_4\text{O}_{12}$  ( $M = 1388.80$  g/mol): triclinic, space group  $P-1$  (no. 2),  $a = 12.0976(13)$  Å,  $b = 16.2812(9)$  Å,  $c = 17.5121(16)$  Å,  $\alpha = 98.439(5)^\circ$ ,  $\beta = 107.408(7)^\circ$ ,  $\gamma = 95.705(6)^\circ$ ,  $V = 3217.9(5)$  Å<sup>3</sup>,  $Z = 2$ ,  $T = 170(2)$  K,  $\mu(\text{CuK}\alpha) = 3.543$  mm<sup>-1</sup>,  $D_{\text{calc}} = 1.433$  g/cm<sup>3</sup>, 85824 reflections measured ( $5.382^\circ \leq 2\theta \leq 139.604^\circ$ ), 11981 unique ( $R_{\text{int}} = 0.0423$ ,  $R_{\text{sigma}} = 0.0283$ ) which were used in all calculations. The final  $R_1$  was 0.0376 ( $I > 2\sigma(I)$ ) and  $wR_2$  was 0.0921 (all data).

### 2.3. Hirshfeld Surface Analysis

Crystal Explorer version 17.5 was used to generate Hirshfeld surfaces and the corresponding 2-D fingerprint plots [18]. The Hirshfeld surfaces of both conformations have been mapped over  $d_{\text{norm}}$  (range  $-0.3$  Å to  $3.6$  Å) and curvedness. The red to blue colour scheme on the Hirshfeld surfaces mapped with  $d_{\text{norm}}$  highlights the shorter and the longer contacts, respectively. The Hirshfeld surface mapped with curvedness can be employed to

examine the effect of weak intermolecular interactions in a crystal. The 2-D fingerprint plots illustrate the summary of the frequency of each combination of  $d_e$  and  $d_i$  across the Hirshfeld surface of a molecule, where  $d_e$  is the distance of an atom external to the generated surface and  $d_i$  is the distance of an atom internal to the surface. Different contributions of interatomic contacts are reflected with different colors, increasing contributions from blue to green to red. The intermolecular interaction energies are calculated in Crystal Explorer version 17.5 from a single point molecular wavefunction at the HF/3-21G level, using a cluster of 3.8 Å radius.

### 3. Results

#### 3.1. Structural Description

Compound **1** crystallises in the triclinic space group  $P-1$  with two molecules present in the asymmetric unit (Figure 3). One of these molecules adopts the partial cone conformation (**1a**), which is characterised by three of the aromatic rings pointing up and one group (more specifically, one of the *p*-benzoquinone moieties) pointing down (Figure 4a). The other molecule in the asymmetric unit (**1b**) adopts the 1,3-alternate conformation, where the *p*-benzoquinone moieties both point in the same direction but in the opposite direction to the brominated aromatic rings (Figure 4b). As the two molecules are simply conformational isomers, it was not surprising to find that there was little difference in the bond lengths found within **1a** and **1b**.

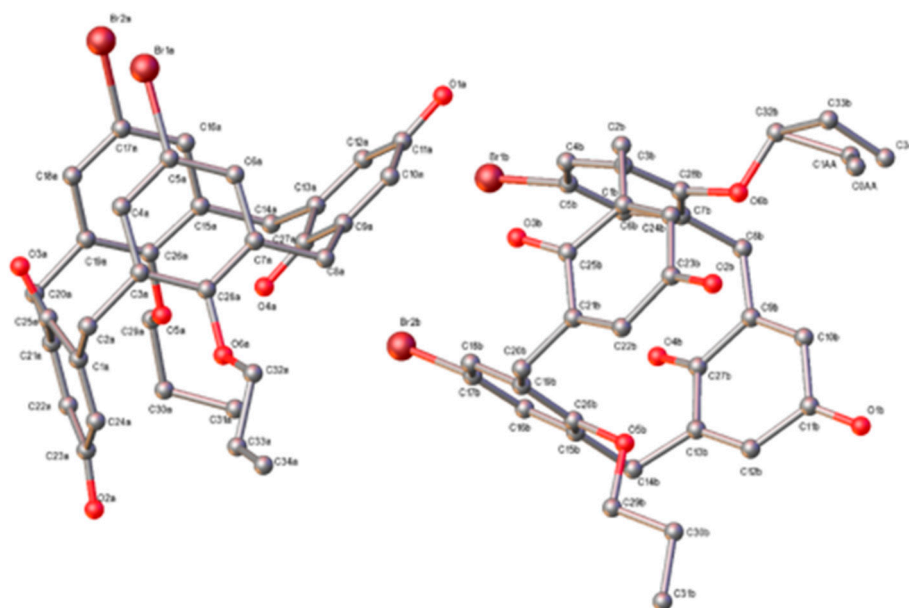


**Figure 3.** Asymmetric unit found in the single crystal X-ray structure of **1**. Hydrogen atoms have been omitted for clarity. One lower-rim propoxy group is disordered over two positions and has been successfully modelled at partial occupancies.

In both **1a** and **1b**, the *p*-benzoquinone moieties are not strictly planar, with the C=O bonds bending outwards, away from the calix[4]diquinone. For comparison, examination of the crystal structure of *p*-benzoquinone itself reveals that it is almost completely planar, with less than 1° deviation from a perfectly planar structure [19]. In **1a**, the *p*-benzoquinone moiety that is orientated downwards exhibits significant deviation from a planar structure: the C24a-C1a-C25a-O3a and C1a-C24a-C23a-O2a dihedral angles have values of 165.8(3)° and −170.7(3)° respectively. This deviation from planar is less in the other *p*-benzoquinone moiety in **1a** (the group orientated upwards), where the O4a-C27a-C9a-C10a and O1a-C11a-C10a-C9a dihedral angles have values of 176.4(2)° and 176.1(3)° respectively. With **1b**, both *p*-benzoquinone moieties exhibit similar deviations from planar. This is most apparent with the C10b-C9b-C27b-O4b torsion angle which has a value of −161.6°. The distortion of the

*p*-benzoquinone structure is a common trait amongst calix[4]diquinone crystal structures. For example, a structurally similar calix[4]diquinone reported by Reddy et al. (YEHVIQ) also exhibits up to 17.0° deviation from being planar [20].

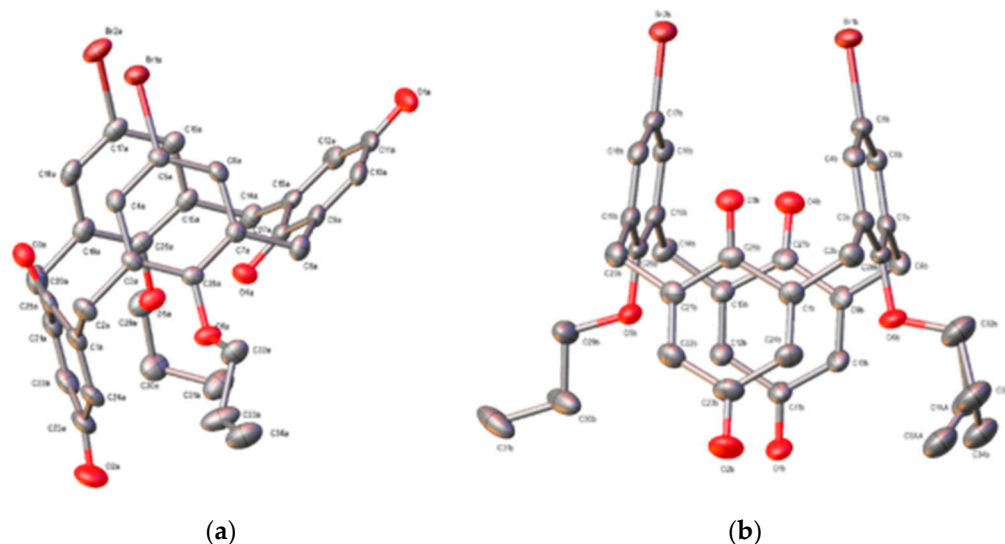


**Figure 4.** Alternative projections (relative to Figure 3) showing ellipsoid plots of the molecular structure of **1a** (a) and **1b** (b). Hydrogen atom and other conformers from the asymmetric unit in **1** have been removed for clarity in each case. Thermal ellipsoids shown at 50% probability.

Unlike other calix[4]arene type structures, which generally have the *para*-substituent (see R group, Figure 1) orientated outwards, both **1a** and **1b** exhibit “pinching” of the bromine atoms towards each other. The intramolecular Br—Br distances in **1a** and **1b** (3.7851(6) and 3.9862(6) Å) are significantly less than in the analogous 5,17-dibromo-26,28-di-*n*-propoxy-25,27-dihydroxycalix[4]arene, where the Br—Br distance is 8.9824(9) Å [21].

Although two conformations of **1** are present in the crystal structure, <sup>1</sup>H and <sup>13</sup>C NMR spectra (see supplementary materials) indicate that only a single conformation was present in solution. Based on the number of peaks present and the symmetry of the four possible conformations, both the partial cone and 1,2-alternate conformations could be ruled out as the single conformation present. Based on the peaks observed in the <sup>13</sup>C NMR, it was postulated that the cone conformation, **1c**, was present [22,23], which is in line with previous conclusions drawn by van Loon et al. into a structurally similar calix[4]diquinone structure [13]. The presence of the two conformers **1a** and **1b** in the crystal structure, and **1c** in solution would suggest that **1** can readily interconvert between the conformations, most likely by an oxygen through the annulus mechanism,[24] and that solid state effects drive crystallization in the present form. This solution phase flexibility is in line with previous reports that calix[4]diquinones are generally more flexible than structurally similar 25,27-dialkoxycalix[4]arenes [11]. An example of this is provided by further comparison of **1** with the analogous 5,17-dibromo-26,28-di-*n*-propoxy-25,27-dihydroxycalix[4]arene (SITTOH), which shows that the latter adopts a single conformation both in solution and in the crystal structure [21].

### 3.2. Crystal Packing and Hirshfeld Surfaces

In the extended structure of **1**, both the two conformers **1a** and **1b** pack side by side along the *a*-axis direction with each independent conformer arranged in alternating layer and belongs to two different packing patterns (Figure 5). A comparable phenomenon was noted for the cyclic alkoxy-organotellurium trihalides where two independent molecules belong to two different packing motifs [25]. The closest contact between molecules of **1a** and **1b** caused by this arrangement involves strong hydrogen bonding between carbonyl O-atoms with adjacent H-atoms, C=O---HC: O11---H10A = 2.292 Å, O4A---H34E = 2.425 Å;

O3A---H34B = 2.516 Å, O2A---H24B = 2.679 Å; O1A and the protons H4B (C-H---O = 2.495(3) Å) and H2BB (C-H---O = 2.892(3) Å). There are also additional interactions between **1a** and **1b** through interaction of the propyl groups with the carbonyl groups, with the H31B---O3A distance of 2.928(5) Å. Furthermore, there are long range interactions involving the bromine atoms, varying in length from 3.119(3) Å for the Br2B---H14C contact to 4.354(3) Å for the Br1B---H14D interaction. Within the layer comprising conformers **1a**, the calixarenes are involved in H-bonding between themselves through the adjacent propoxy chains with C33A-H33D---O6A distance measured at 2.60 Å while for layer comprising conformers **1b**, the neighbouring calixarenes are engaged in the offset face-to-face interaction involving the phenyl rings with C--- $\pi_{(\text{centroid})}$  distance at 3.83 Å. In the direction of the *a*-axis, the extended structure is characterized by molecules of either **1a** or **1b** packing in an up-down antiparallel bilayer arrangement (Figure 6a,b) which is common for calix[4]arenes. Additionally, some protons are oriented towards the C=C bond plane (plane of the benzene ring) and form CH--- $\pi$  bonds with average distances of  $2.75 \pm 0.10$  Å, coinciding with the CH--- $\pi$  bond distances as reported by Nishio [26].

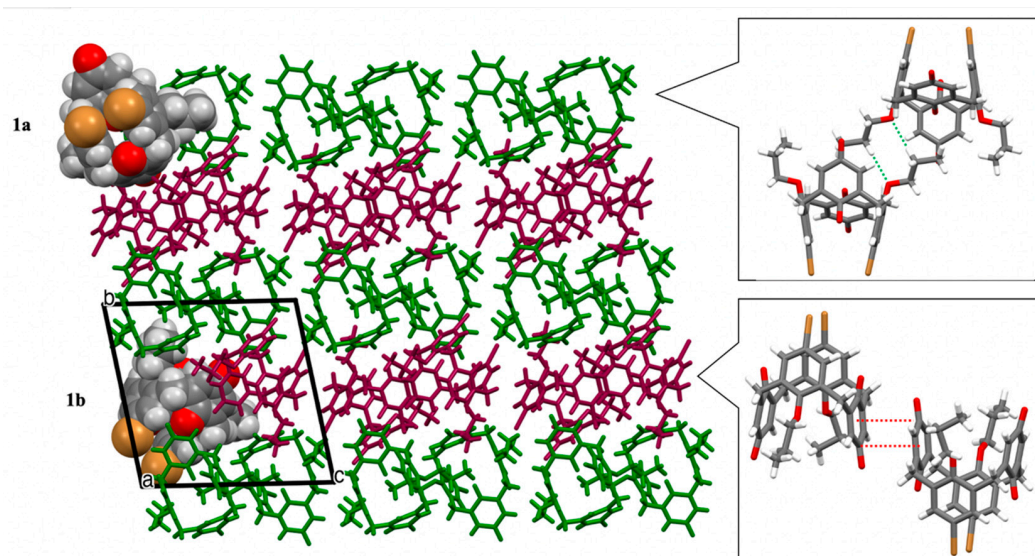


**Figure 5.** Packing of **1** viewed along the *a*-axis direction, showing alternating layers of conformers **1a** (green) and **1b** (maroon). Inset: The intermolecular interactions of adjacent calixarenes within the layers of conformers **1a** and **1b**.

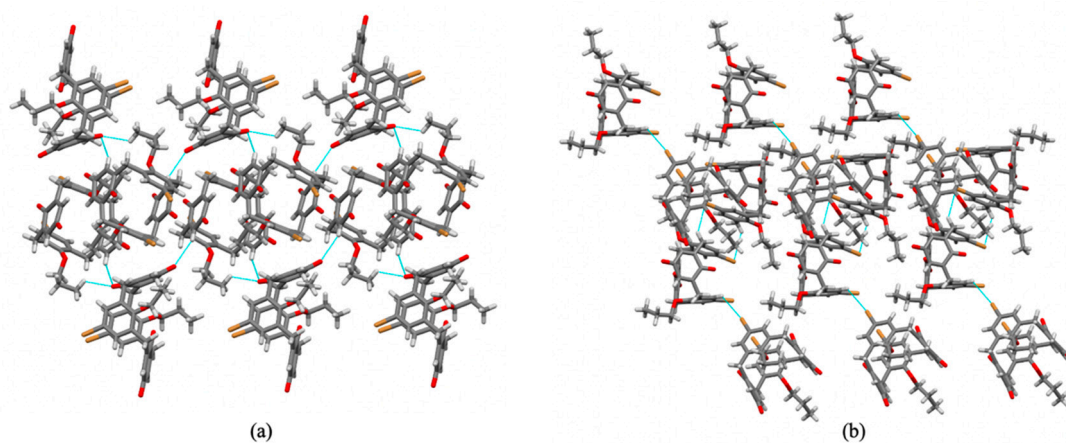


**Figure 6.** Crystal packing showing (a) the C=O---H-C interactions (blue lines) involving **1a** and **1b** and (b) close Br---H-C networks (blue lines) between **1a** and **1b**.

It is observed that the Hirshfeld surface analysis of **1a** and **1b** contains the highest proportion of H···H interactions (44.1% and 44.5%, respectively), as this is consistent with the high proportion of hydrogen atoms in the molecular structure (Figures 7 and 8). There is a form of pairwise O···H interaction present, comprising 20.1% and 22.9% of the Hirshfeld surface for **1a** and **1b**, respectively, and this results in the appearance of two spikes corresponding to both the donor and acceptor of C–H···O hydrogen bonds in the fingerprint plots delineated into O···H/H···O contacts. Intense circular depressions (red spots) are found on the Hirshfeld surfaces indicating hydrogen bond interactions (Figure 9). The smaller proportion of O···H interaction results in a larger proportion of H···Br interaction for **1a**, however, the opposite trend was seen for **1b** where H···Br interaction make up 11.5% of the Hirshfeld surface. The Hirshfeld surfaces mapped over  $d_{\text{norm}}$  also shows the contribution of the medium range contact i.e., the donor and the acceptors intermolecular C–H··· $\pi$  contacts (C–H··· $\pi$ / $\pi$ ···H–C; often abbreviated as C···H/H···C), accounting for 11.8% and 12.1% of the surface for **1a** and **1b**, respectively.

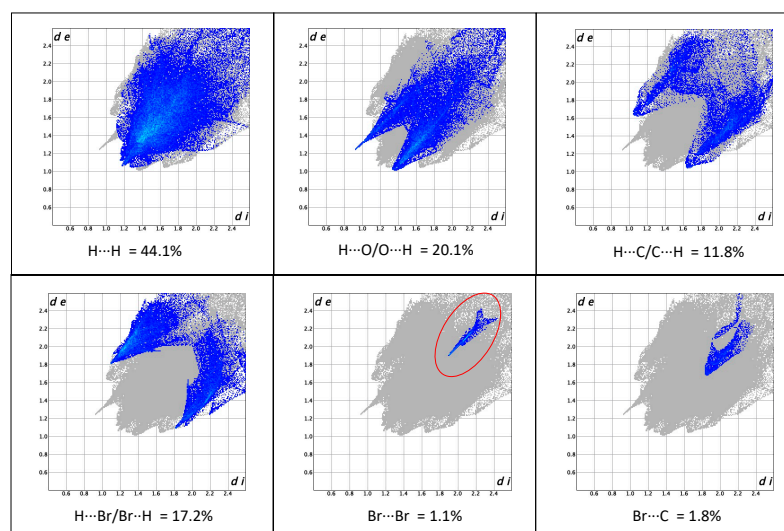


**Figure 7.** Fingerprint plots for **1a**, delineated into H···H, O···H/H···O, C···H/H···C, Br···H/H···Br, Br···Br and Br···C contacts.

It is noteworthy that Hirshfeld surface analysis is extremely useful for identifying other interactions (notably relatively weaker interactions) apart from the conventional interactions such as C–H···O and C–H··· $\pi$ . We have carefully examined the halogen bond interaction and found that the halogen bond is very closely related to the type-II interaction with  $\theta_1 \approx 92^\circ$  (C17B–Br2B···Br2A) and  $\theta_2 \approx 160^\circ$  (C17A–Br2A···Br2B) as a consequence of close packing [27]. We note that although only 1.1% of the surface is assigned to Br···Br contact for both **1a** and **1b**, a bright streak is still visible at the top right of the fingerprint plot, circled in red in Figures 7 and 8. Interestingly, the presence of Br···Br contact is visible on the Hirshfeld surface when mapped over curvedness (Figure 10). This relatively low percentage solely relates to the proportion of interactions within the crystal structure (given that there is only two Br per molecule, the contribution to the surface will generally be low) and does not reflect the strength of such interaction on the solid-state behavior. The remaining contributions to the Hirshfeld surface are from the Br···C (shortest contact at 3.65 Å for Br1B···C18A) at and O···C (shortest contact at 3.11 Å for O3A···C34B) contacts making up only 1.8% and 3.2% to the surface for **1a** while 1.7% and 4.3% for **1b**.

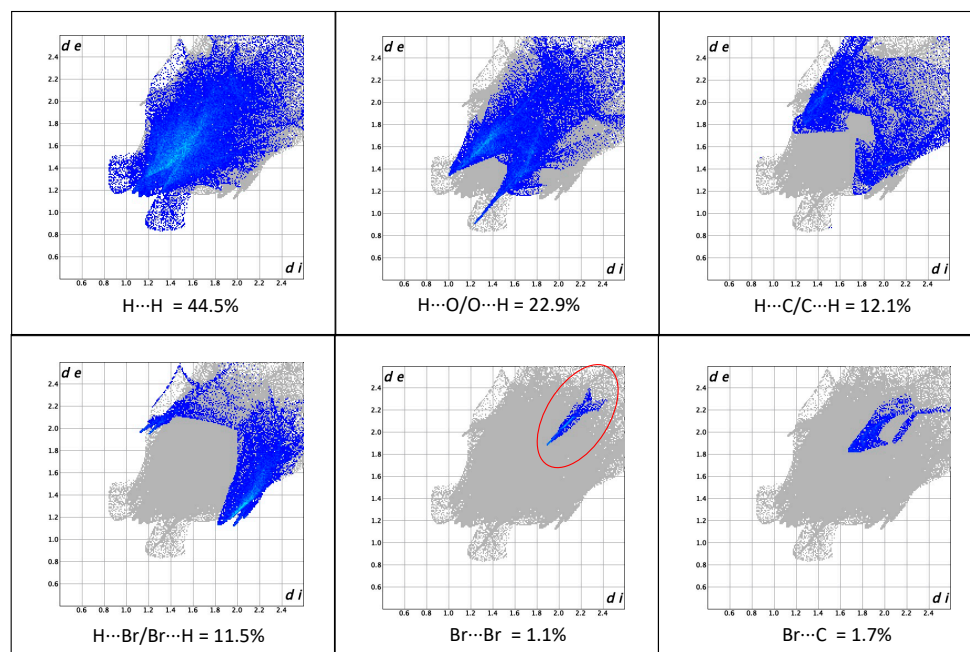


**Figure 8.** Fingerprint plots for **1b**, delineated into H...H, O...H/H...O, C...H/H...C, Br...H/H...Br, Br...Br and Br...C contacts.

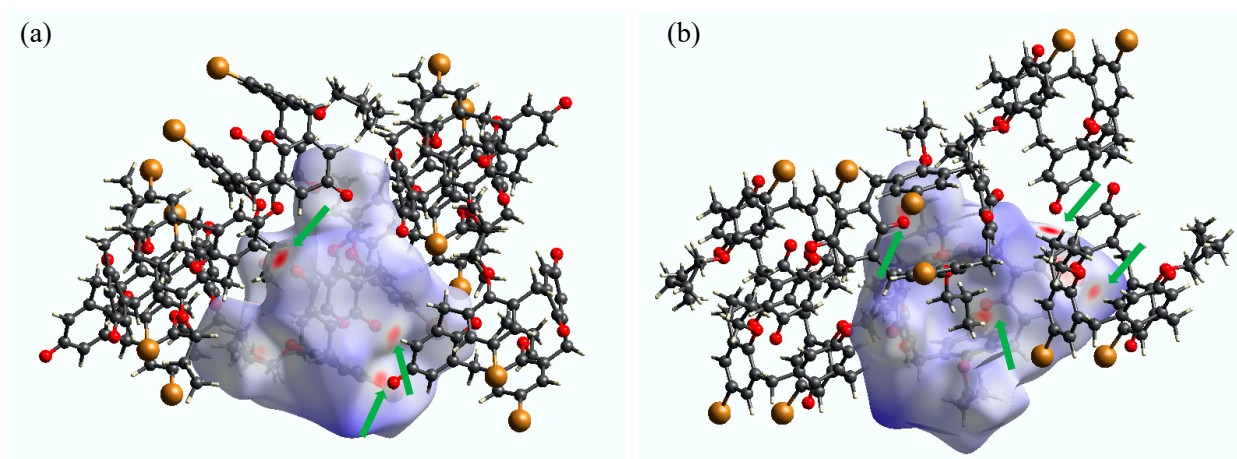


**Figure 9.** The  $d_{\text{norm}}$  surfaces for **1a** (a) and **1b** (b) showing C–H...O interactions (red spots with green arrow).

We have also used CrystalExplorer to calculate the intermolecular interaction energies using the CE–HF/3-21G energy model [18] to visualize the interaction topology in the crystal structures. The energy frameworks for electrostatic, dispersion, and total energy components are shown in red, green, and blue colored tubes, as shown in Figure 11. All the frameworks were adjusted to the same cylinder scale factor of 150. The relative strengths of the overall packing interaction energy are indicated by the cylindrical shapes where the radius of the rods is proportional to the magnitude of the interaction energy. The total intermolecular energy is the sum of electrostatic, polarization, dispersion, and exchange-repulsion energies [28] with scale factors of 1.019, 0.651, 0.901, and 0.811, respectively [29]. From the energy framework analysis, we found that the dispersion contribution dominates in the intermolecular interactions. The two alternating calixarene layers of different conformers give the parallel cylindrical tubes when viewed down the *c*-axis with a larger diameter for the total energy ( $-89.1 \text{ kJ mol}^{-1}$ ) and dispersion ( $-57.0 \text{ kJ mol}^{-1}$ ) components ascribed for the same type of conformer that self-interact strongly within themselves while

the smaller tube diameter intersecting calixarene layers of different conformers illustrates the weaker contribution of the dispersion ( $-25.8 \text{ kJ mol}^{-1}$ ) component yielding the total energy of  $-31.3 \text{ kJ mol}^{-1}$ .

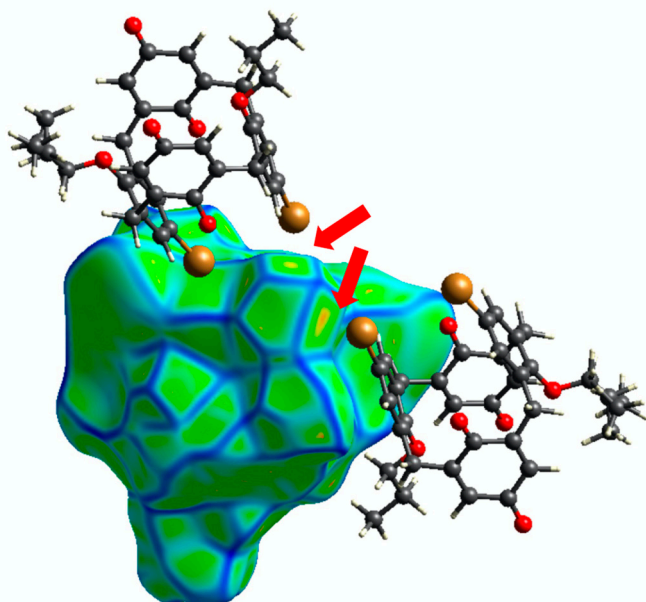


**Figure 10.** The Hirshfeld surface mapped over curvedness highlighting the weak Br...Br contact red arrows.

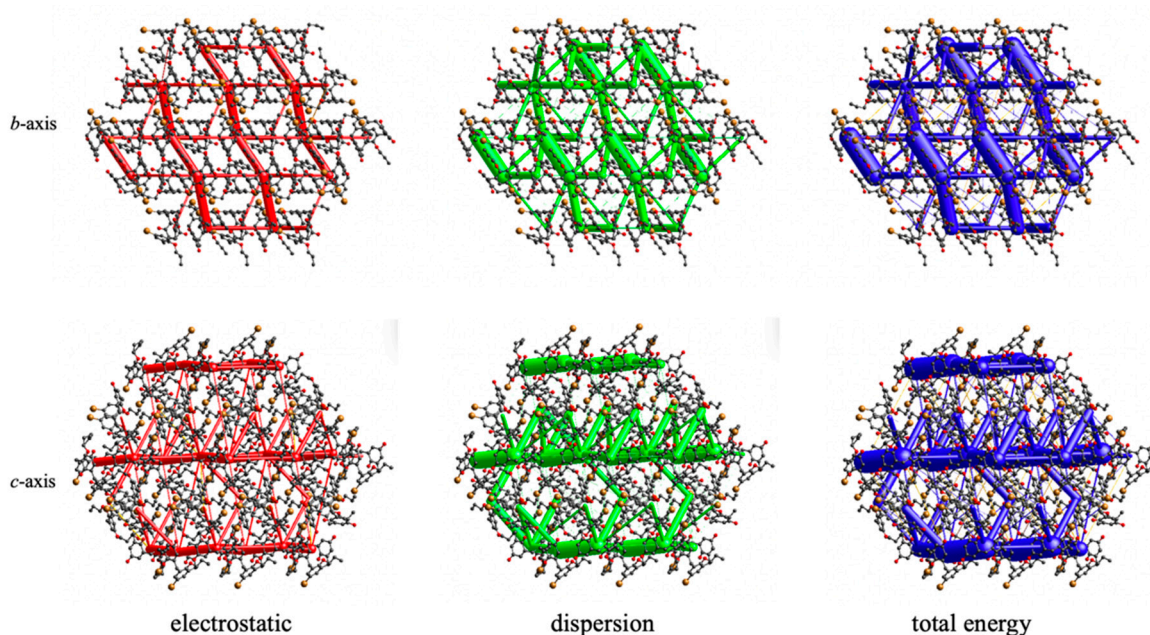


**Figure 11.** Energy-framework diagrams for  $E_{ele}$ ,  $E_{dis}$  and  $E_{tot}$  for a cluster of molecules in the crystal structure of **1** along *b*- and *c*-axes.

#### 4. Discussion

Following this analysis, the Cambridge Structural Database (CSD, Version 5.41, updated March 2020) [30] was searched for diametrically symmetrical calix[4]diquinones. This returned a total of 41 results, of which 29 were metal-calix[4]quinone complexes and lower-rim bridged calix[4]quinones. These are unsuitable for comparison with **1** because the metal binding/lower-rim bridges would dramatically influence the conformational

flexibility of the calix[4]quinone. Of the remaining 12 structures, a total of seven hits had simple alkyl chains on the lower rim (NUPHUB, NUPHUB01, PETDOH, PETDUN, PETFAV, VUSNED, and YEHVIQ) [11,20,31,32]. A common structural theme amongst these seven crystal structures and **1** was the deviation of the *p*-benzoquinone moieties from a perfectly planar structure. Amongst these structures, the prevalent conformation was the partial-cone conformation, however, in each case, only a single conformation was present in the asymmetric unit. The best structural comparison to the **1** is provided by YEHVIQ, which differs structurally in that both bromine atoms are replaced with *tert*-butyl groups, with only the 1,3-alternate conformation present [20].

A wider examination of the CSD revealed that the occurrence of multiple conformations of calix[4]arene-type structures within a single asymmetric unit is extremely rare, but not unprecedented. A search for structures possessing the basic calix[4]arene skeleton with the additional criteria that more than one molecule must be present in the asymmetric unit ( $Z' > 1$ ) yielded a total of 332 results. Any results that featured metal binding/lower-rim bridges or possessed multiple molecules with the same conformation were discounted, leading to only a single target structure (IWESAF) [33]. This crystal structure of 5,11,17,23-tetra-*t*-butyl-26,28-dihydroxy-25,27-dimethoxycalix[4]arene featured both the cone and partial cone conformations within the asymmetric unit. Expanding the search to also include any atoms on the methylene bridge positions yielded a thiacalix[4]arene (CH<sub>2</sub> bridges replaced by sulfur atoms) as an additional structure (ALETEQ) [34]. Three molecules were present in the asymmetric unit of this structure, with two molecules adopting the cone conformation while the final one adopted the 1,3-alternate conformation.

## 5. Conclusions

In conclusion, the crystal structure of 5,17-dibromo-11,27,23,25-tetraone-26,28-dipropoxycalix[4]arene, **1**, is reported and exhibits the highly unusual feature of containing two different conformations, partial cone, and 1,3-alternate, of the same molecule within the asymmetric unit. A search of the CSD returns only two other calix[4]arene type structures exhibiting this property, showing that such observations are rare. The behaviour of **1** in the solid state varies drastically from that in solution, where only the cone conformation was found to be present. This also suggests that calix[4]diquinones are more conformationally flexible relative to their other structurally analogous calix[4]arenes, which would be locked into a single atropisomer. This may have a downstream impact in understanding how such molecules react in subsequent synthetic reactions, particularly in the solid state, and work in this area will be reported in due course.

**Supplementary Materials:** The following are available online at <https://www.mdpi.com/article/10.3390/cryst12020250/s1>, Figure S1: <sup>1</sup>H NMR spectra of **1**, Figure S2: <sup>13</sup>C NMR spectra of **1**, Figure S3: IR spectra of **1**.

**Author Contributions:** Conceptualization, D.T. and S.J.D.; methodology, D.T. and S.J.D.; validation, D.T. and S.J.D.; formal analysis, D.T., I.L. and S.J.D.; investigation, D.T. and S.J.D.; resources, F.V. and S.J.D.; data curation, D.T. and S.J.D.; writing—original draft preparation, D.T. and I.L.; writing—review and editing, I.L., F.V. and S.J.D.; visualization, I.L., F.V. and S.J.D.; supervision, F.V. and S.J.D.; project administration, D.T., F.V. and S.J.D.; funding acquisition, F.V. and S.J.D. All authors have read and agreed to the published version of the manuscript.

**Funding:** This research was funded by the EPSRC, grant number EP/L016419/1.

**Institutional Review Board Statement:** Not applicable.

**Informed Consent Statement:** Not applicable.

**Data Availability Statement:** The Crystallographic Information File (CIF) for **1** (CCDC 2132914) has been deposited in the CCDC database and can be accessed through <https://www.ccdc.cam.ac.uk/structures/> (accessed on 8 January 2022).

**Conflicts of Interest:** The authors declare no conflict of interest.

## References

1. Suga, K.; Fujihira, M.; Morita, Y.; Agawa, T. Electrochemical study on calix[4]quinone and calix[4]hydroquinone in *N,N*-dimethylformamide. *J. Chem. Soc. Faraday Trans.* **1991**, *87*, 1575–1578. [CrossRef]
2. Genorio, B. The synthesis of diquinone and dihydroquinone derivatives of calix[4]arene and electrochemical characterization on Au(111) surface. *Acta Chim. Slov.* **2016**, *63*, 496–508. [CrossRef]
3. Pirnat, K.; Dominko, R.; Cerc-Korosec, R.; Genorio, B.; Gaberscek, M. Electrochemically stabilised quinone based electrode composites for Li-ion batteries. *J. Power Sources* **2012**, *199*, 308–314. [CrossRef]
4. Huang, W.; Zhu, Z.; Wang, L.; Wang, S.; Li, H.; Tao, Z.; Shi, J.; Guan, L.; Chen, J. Quasi-solid-state rechargeable lithium-ion batteries with a calix[4]quinone cathode and gel polymer electrolyte. *Angew. Chem. Int. Ed.* **2013**, *52*, 9162–9166. [CrossRef] [PubMed]
5. Kang, S.K.; Lee, O.S.; Chang, S.K.; Chung, D.S.; Kim, H.; Chung, T.D. Calcium ion-Calixquinone complexes adsorbed on a silver electrode. *J. Phys. Chem. C* **2009**, *113*, 19981–19985. [CrossRef]
6. Kim, Y.R.; Kim, R.S.; Kang, S.K.; Choi, M.G.; Kim, H.Y.; Cho, D.; Lee, J.Y.; Chang, S.K.; Chung, T.D. Modulation of quinone PCET reaction by Ca<sup>2+</sup> ion captured by calix[4]quinone in water. *J. Am. Chem. Soc.* **2013**, *135*, 18957–18967. [CrossRef]
7. Lee, M.-D.; Yang, K.-M.; Tsoo, C.-Y.; Shu, C.-M.; Lin, L.-G. Calix[4]quinone. Part 1: Synthesis of 5-hydroxycalix[4]arene by calix[4]quinone monoketal route. *Tetrahedron* **2001**, *57*, 8095–8099. [CrossRef]
8. Gutsche, C.D.; Bauer, L.J. Calixarenes. 13. The conformational properties of calix[4]arenes, calix[6]arenes, calix[8]arenes, and oxacalixarenes. *J. Am. Chem. Soc.* **1985**, *107*, 6052–6059. [CrossRef]
9. Gutsche, C.D.; Levine, J.A. Calixarenes. 6. Synthesis of a functionalizable calix[4]arene in a conformationally rigid cone conformation. *J. Am. Chem. Soc.* **1982**, *104*, 2652–2653. [CrossRef]
10. Gutsche, C.D. Embroidering the baskets: Modifying the upper and lower rims of calixarenes. In *Calixarenes Revisited*; Gutsche, C.D., Ed.; Royal Society of Chemistry: Cambridge, UK, 1998; pp. 79–145.
11. Casnati, A.; Comelli, E.; Fabbri, M.; Bocchi, V.; Pochini, A.; Ungaro, R.; Mori, G.; Ugozzoli, F.; Lanfredi, A.M.M. Synthesis, conformations and redox properties of diametrical calix[4]arenequinones. *Recl. Des Trav. Chim. Des Pays-Bas* **1993**, *112*, 384–392. [CrossRef]
12. McKillop, A.; Perry, D.H.; Edwards, M.; Antus, S.; Farkas, L.; Nogradi, M.; Taylor, E.C. Thallium in organic synthesis. XLII. Direct oxidation of 4-substituted phenols to 4,4-disubstituted cyclohexa-2,5-dienones using thallium(III) nitrate. *J. Org. Chem.* **1976**, *41*, 282–287. [CrossRef]
13. Van Loon, J.D.; Arduini, A.; Coppi, L.; Verboom, W.; Pochini, A.; Ungaro, R.; Harkema, S.; Reinhoudt, D.N. Selective functionalization of calix[4]arenes at the upper rim. *J. Org. Chem.* **1990**, *55*, 5639–5646. [CrossRef]
14. Gutsche, C.D.; Pagoria, P.F. Calixarenes. 16. Functionalized calixarenes: The direct substitution route. *J. Org. Chem.* **1985**, *50*, 5795–5802. [CrossRef]
15. Dolomanov, O.V.; Bourhis, L.J.; Gildea, R.J.; Howard, J.A.K.; Puschmann, H. OLEX2: A complete structure solution, refinement and analysis program. *J. Appl. Crystallogr.* **2009**, *42*, 339–341. [CrossRef]
16. Sheldrick, G.M. SHELXT-Integrated space-group and crystal-structure determination. *Acta Crystallogr. Sect. A Found. Crystallogr.* **2015**, *71*, 3–8. [CrossRef] [PubMed]
17. Sheldrick, G.M. Crystal structure refinement with SHELXL. *Acta Crystallogr. Sect. C Struct. Chem.* **2015**, *71*, 3–8. [CrossRef] [PubMed]
18. Turner, M.J.; McKinnon, J.J.; Wolff, S.K.; Grimwood, D.J.; Spackman, P.R.; Jayatilaka, D.; Spackman, M.A. CrystalExplorer17. University of Western Australia. 2017. Available online: <http://hirshfeldsurface.net> (accessed on 8 January 2022).
19. Trotter, J. A three-dimensional analysis of the crystal structure of *p*-benzoquinone. *Acta Crystallogr.* **1960**, *13*, 86–95. [CrossRef]
20. Kennedy, S.R.; Main, M.U.; Pulham, C.R.; Ling, I.; Dalgarno, S.J. A self-assembled nanotube supported by halogen bonding interactions. *CrystEngComm* **2019**, *21*, 786–790. [CrossRef]
21. Jaime, C.; De Mendoza, J.; Prados, P.; Nieto, P.M.; Sanchez, C. Carbon-13 NMR chemical shifts. A single rule to determine the conformation of calix[4]arenes. *J. Org. Chem.* **1991**, *56*, 3372–3376. [CrossRef]
22. Eddaif, L.; Shaban, A.; Telegdi, J. Sensitive detection of heavy metals ions based on the calixarene derivatives-modified piezoelectric resonators: A review. *Int. J. Environ. Anal. Chem.* **2019**, *99*, 824–853. [CrossRef]
23. Otsuka, H.; Shinkai, S. Stereochemical control of calixarenes useful as rigid and conformationally diversiform platforms for molecular design. *Supramol. Sci.* **1996**, *3*, 189–205. [CrossRef]
24. Torubaev, Y.V.; Skabitsky, I.V. Crystals at a Carrefour on the Way through the Phase Space: A Middle Path. *Molecules* **2021**, *26*, 1583. [CrossRef] [PubMed]
25. Desiraju, G.R.; Parthasarathy, R. The Nature of Halogen···Halogen Interactions: Are Short Halogen Contacts Due to Specific Attractive Forces or Due to Close Packing of Nonspherical Atoms? *J. Am. Chem. Soc.* **1989**, *111*, 8725–8726. [CrossRef]
26. Nishio, M. The CH/π hydrogen bond in chemistry. Conformation, supramolecules, optical resolution and interactions involving carbohydrates. *Phys. Chem. Chem. Phys.* **2011**, *13*, 13873–13900. [CrossRef]
27. Turner, M.J.; Thomas, S.P.; Shi, M.W.; Jayatilaka, D.; Spackman, M.A. Energy frameworks: Insights into interaction anisotropy and the mechanical properties of molecular crystals. *Chem. Commun.* **2015**, *51*, 3735–3738. [CrossRef]
28. Mackenzie, C.F.; Spackman, P.R.; Jayatilaka, D.; Spackman, M.A. CrystalExplorer model energies and energy frameworks: Extension to metal coordination compounds, organic salts, solvates and open-shell systems. *IUCr* **2017**, *4*, 575–587. [CrossRef]

29. Groom, C.R.; Bruno, I.J.; Lightfoot, M.P.; Ward, S.C. The Cambridge Structural Database. *Acta Crystallogr. Sect. B Struct. Sci. Cryst. Eng. Mater.* **2016**, *72*, 171–179. [[CrossRef](#)]
30. Beer, P.D.; Gale, P.A.; Chen, Z.; Drew, M.G.B.; Heath, J.A.; Ogden, M.I.; Powell, H.R. New Ionophoric Calix[4]diquinones: Coordination Chemistry, Electrochemistry, and X-ray Crystal Structures. *Inorg. Chem.* **1997**, *36*, 5880–5893. [[CrossRef](#)]
31. Meddeb-Limem, S.; Besbes-Hentati, S.; Said, H.; Malezieux, B.; Chamoreau, L.M.; Bouvet, M. Electrosynthesis and Structural Studies of 5,17-Di-*tert*-butyl-26,28-dimethoxycalix[4]arene-25,27-diquinone. *X-ray Struct. Anal. Online* **2010**, *26*, 29–30. [[CrossRef](#)]
32. Reddy, P.A.; Kashyap, R.P.; Gutsche, C.D.; Watson, W.H. Watson CCDC 158880: Experimental Crystal Structure Determination. 2001. Available online: <https://www.ccdc.cam.ac.uk/structures/search?id=doi:10.5517/cc5bb5z&sid=DataCite> (accessed on 8 January 2022). [[CrossRef](#)]
33. Fischer, C.; Gruber, T.; Eissmann, D.; Seichter, W.; Weber, E. Unusual Behavior of a Calix[4]arene Featuring the Coexistence of Basic Cone and 1,2-Alternate Conformations in a Solvated Crystal. *Cryst. Growth Des.* **2011**, *11*, 1989–1994. [[CrossRef](#)]
34. Lhoták, P.; Himl, M.; Stibor, I.; Sýkora, J.; Dvořáková, H.; Lang, J.; Petříčková, H. Conformational behaviour of tetramethoxythiacalix[4]arenes: Solution versus solid-state study. *Tetrahedron* **2003**, *59*, 7581–7585. [[CrossRef](#)]